HHS Public Access

Author manuscript

Neuroscience. Author manuscript; available in PMC 2017 February 09.

Published in final edited form as:

Neuroscience. 2016 February 9; 314: 35–46. doi:10.1016/j.neuroscience.2015.11.048.

Role of Estradiol in Intrinsic Hindbrain AMPK Regulation of Hypothalamic AMPK, Metabolic Neuropeptide, and Norepinephrine Activity and Food Intake in the Female Rat

Fahaad S.H. Alenazi, **Baher A. Ibrahim**, **Hussain Al-Hamami**, **Manita Shakiya**, and **Karen P. Briski**

Department of Basic Pharmaceutical Sciences, School of Pharmacy, The University of Louisiana at Monroe, Monroe, LA 71201

Abstract

This study addressed the hypothesis that dorsomedial hindbrain adenosine 5'-monophosphate-activated protein kinase (AMPK) imposes inherent control over hypothalamic AMPK, neuropeptide, and norepinephrine (NE) activity and governs feeding in an estradiol-dependent manner. Groups of estradiol (E)- or oil (O)-implanted ovariectomized rats were injected with the AMPK inhibitor Compound C (Cc) or vehicle into the caudal fourth ventricle (CV4) prior to micropunch-dissection of individual hypothalamic metabolic loci or assessment of food intake. Cc decreased hindbrain dorsal vagal complex phosphoAMPK (pAMPK) profiles in both E and O; tissue ATP levels were reduced by this treatment in O only. In E/Cc, pAMPK expression was diminished in the lateral hypothalamic area (LHA) and ventromedial (VMH) and paraventricular (PVH) nuclei; only PVH pAMPK was suppressed by this treatment in O/Cc. Cc decreased PVH corticotropin-releasing hormone and arcuate (ARH) proopiomelanocortin (POMC) and neuropeptide Y in O, but suppressed only POMC in E. O/Cc exhibited both augmented (PVH, VMH) and decreased (LHA, ARH) hypothalamic NE content, whereas Cc treatment of E elevated preoptic and dorsomedial hypothalamic nucleus NE. Cc completely or incompletely repressed feeding in E versus O, respectively. Results implicate dorsomedial hindbrain AMPK in physiological stimulus-induced feeding in females. Excepting POMC, hypothalamic neuropeptide targets of input from that sensor may differ in presence vs. absence of estrogen. Estradiol likely determines hypothalamic targets of altered NE signaling due to hindbrain AMPK activation. Divergent changes in NE content of hypothalamic loci in O/Cc uniquely demonstrate sensor-induced bimodal catecholamine signaling to those sites.

Correspondence: Dr. Karen P. Briski, Ph.D., Professor of Pharmacology and Neuroanatomy, Head, Department of Basic Pharmaceutical Sciences, School of Pharmacy, College of Health and Pharmaceutical Sciences, The University of Louisiana at Monroe, 356 Bienville Building, 1800 Bienville Drive, Monroe, LA 71201, TEL: 318-342-3283, FAX: 318-342-1737, briski@ulm.edu.

Keywords

Compound C; estradiol; adenosine 5'-monophosphate-activated protein kinase; ATP; norepinephrine; pro-opiomelanocortin

Introduction

The ultrasensitive, evolutionarily-conserved energy gauge adenosine 5'-monophosphate-activated protein kinase (AMPK) provides crucial input on brain cell ATP availability to neural pathways that control whole-body energy stability. AMPK is activated via phosphorylation in response to metabolic stressors (exercise, starvation, hypoxia, etc.) that increase the intracellular AMP/ATP ratio [Hardie, 2003; Kahn et al., 2005]. Phosphorylated AMPK (pAMPK) inhibits ATP-consuming biosynthetic pathways, while augmenting ATP-producing metabolic pathways such as fatty acid oxidation. AMPK is expressed in hypothalamic and hindbrain elements of the sizable brain metabolic regulatory network. Hindbrain dorsal vagal complex (DVC) AMPK is implicated in neural regulation of feeding [Hayes et al., 2009] and glucostasis [Ibrahim et al., 2013]. DVC AMPK responds to substrate fuel availability as activation of this sensor by insulin-induced hypoglycemia is normalized by localized infusion of the oxidizable glucose metabolite L-lactate [Gujar et al., 2014]. The hypothalamus operates as the final common conduit for control of behavioral, autonomic, and neuroendocrine motor responses to energy imbalance. The capability of hindbrain lactate repletion to reverse hypoglycemic patterns of hypothalamic AMPK activation and metabolic neuropeptide expression [Gujar et al., 2014] implies that hindbrain energy state is a critical cue to hypothalamic metabolic monitoring and effector functions.

The ovarian steroid hormone estradiol regulates metabolic status in female mammals via central and peripheral mechanisms that control energy procurement, ingestion, metabolism, partitioning, storage, and expenditure [Wade and Schneider, 1992]. Evidence that caudal DVC A2 noradrenergic neurons express estrogen receptor-alpha (ERα) and -beta (ERβ) proteins [Ibrahim et al., 2013] as well as biomarkers for metabolic sensing, e.g. glucokinase, K_{ATP}, and AMPK [Briski et al., 2009; Cherian and Briski, 2011; Ibrahim et al., 2013] suggests that these cells are substrates for estrogenic input to neural pathways that control energy homeostasis. Our studies show that estradiol controls A2 hindbrain and hypothalamic AMPK, hypothalamic metabolic neurotransmitter, and physiological and behavioral counter-regulatory responses to intra-caudal fourth ventricular administration of the AMP mimic 5-aminoimidazole-4-carboxamide-riboside (AICAR) in ovariectomized (OVX) female rats [Ibrahim et al., 2013; Alenazi et al., 2014; Ibrahim and Briski, 2014]. Outcomes of that work uniquely establish dependency of hindbrain-hypothalamic AMPK functional interaction on estrogen., as pAMPK expression was elevated in hypothalamic arcuate and parventricular nuclei, but diminished in the ventromedial hypothalamic nucleus in estradiol- versus oil-implanted OVX rats after hindbrain AMPK activation. The present studies extend that research by investigating the hypothesis that intrinsic caudal DVC AMPK activity regulates hypothalamic AMPK function and metabolic neuropeptide expression in an estradiol-dependent manner. Groups of OVX female rats were implanted with subcutaneous estradiol-filled capsules designed to reinstate plasma hormone levels at estrous cycle-like levels, with

or capsules containing vehicle only, prior to caudal fourth ventricular administration of the AMPK inhibitor Compound C (Cc). Individual hypothalamic metabolic loci were microdissected by the Palkovits punch method after drug delivery for measurements of total/phosphorylated AMPK and neuropeptide transmitter levels. Recent findings point to A2 neurons as a principal source of noradrenergic signaling of hypoglycemia-associated adjustments in substrate fuel status from the hindbrain to multiple hypothalamic metabolic loci in male rats [Shrestha et al., 2014]. Here, we examined whether inhibition of caudal DVC AMPK activity alters tissue norepinephrine (NE) levels in those sites, and if estradiol controls the magnitude and/or direction of changes in NE activity in a site-specific manner. Evidence that neural regulation of feeding involves estradiol action on the DVC [Thammacharoen et al., 2008] impelled investigation of the role of this hormone in caudal DVC AMPK regulation of food intake.

Methods and Materials

Animals

Adult female Sprague Dawley rats, 250–300 grams body weight (*bw*) were maintained under a 14 hr-light/10 hr-dark schedule (lights on at 05.00 hr), and allowed free access to standard laboratory rat chow (Harlan Teklad LM-485; Harlan Industries, Madison, WI) and water. Animals were acclimated to daily handling. All experimental protocols were conducted in accordance with NIH guidelines for the care and use of laboratory animals, with approval by the ULM Institutional Animal Care and Use Committee.

Experimental Design

On day 1, animals were implanted with a PE-20 cannula into the caudal fourth ventricle (CV4; coordinates: 6.6 mm ventral to skull surface, 0 mm lateral to midline, 13.3 mm posterior to *bregma*) under ketamine:xylazine anesthesia (0.1 ml/100 g *bw ip*, 90 mg ketamine:10 mg xylazine/ml; Henry Schein, Melville, NY), and transferred to individual cages. On day 7, re-anesthetized rats were bilaterally OVX and implanted *sc* with a silastic capsule (0.062 in. *i.d.* × 0.125 in. *o.d.*; 10 mm/100 g *bw*) filled with the vehicle, safflower oil (O) or 30 μg estradiol benzoate (E)/mL oil [Briski et al., 2001]. This steroid replacement regimen yields approximate plasma E concentrations of 22 pg/mL [Tamrakar et al.,2015], replicating circulating hormone levels characteristic of metestrus in 4-day [Butcher et al., 1974] or of diestrus day-2 in 5-day ovary-intact cycling animals [Goodman, 1978]. Ketoprofen (1 mg/kg *bw sc*) was administered prior to and after each surgery; closed incisions were treated topically with 0.25% bupivicaine (1-3 drops). Food was removed at 21.00 hr (2 hr after lights off) on day 11. On the following day at 09.00 hr (time zero; t_0), groups of E and O rats were injected into the CV4 with Cc [5.0 ug/2.0 uL; Hayes et al., 2009; n=5 O/Cc; n=5 E/Cc] or vehicle (V) (n=5 O/V, n=5 E/V) and sacrificed at 10.00 hr for brain and trunk blood collection. Fore- and hindbrains were snap-frozen in liquid nitrogen-cooled isopentane and stored at −80°C. Individual forebrains were cut into serial 100 μm frozen sections through the preoptic area and hypothalamus. The Palkovits micropunch technique was used to dissect the *anteroventral periventricular nucleus* [AVPV; −0.00 to −0.26 mm]; *medial preoptic nucleus* [MPN; −0.26 to −0.60 mm]; *paraventricular hypothalamic nucleus* [PVH; −1.78 to −2.00 mm]; arcuate hypothalamic nucleus [ARH;

−1.78 to −3.25 mm]; *ventromedial hypothalamic nucleus* [VMH; −2.00 to −3.25 mm]; *dorsomedial hypothalamic nucleus* [DMH; −2.45 to −3.25 mm]; and *lateral hypothalamic area* [LHA; −1.78 to 3.28 mm] over pre-determined rostro-caudal intervals relative to *bregma* [Shrestha et al., 2014]. Tissue samples were obtained using calibrated Palkovits-style hollow punch tools of 0.29 mm- [AVPV], 0.51 mm- [MPN, PVH, ARH, VMH and DMH], or 0.76 mm- [LHA] diameter [prod. no. 57401, Stoelting, Inc., Kiel, WI, USA], using neuroanatomical landmarks depicted in *Brain Maps: Structure of the Rat Brain* (L.W. Swanson, Elsevier, 1999) as a guide. This approach created, for each animal, two tissue sample pools for each preoptic/hypothalamic structure of interest. Pooled tissue from one hemi-forebrain was used for Western blot analysis of neuropeptide expression; sample pools from the other half-forebrain were evaluated by ELISA methods for NE content. The hindbrain caudal dorsal vagal complex (cDVC) was bilaterally micropunched (using a 0.76 mm-diameter needle) from two consecutive 200 μm frozen sections cut beginning at −14.40 mm posterior to *bregma*. For each animal, punches from one side of the cDVC were pooled and evaluated by Western blot, while tissue from the remaining side was saved for ATP analysis. Additional groups of animals were acclimated to the presence and regular removal of standard laboratory rat chow in food jars inside their home cages for three consecutive days (days 9-11) prior to feeding analyses on day 12. Food was removed from E and O rats at 21.00 hr on day 11; other animals (full-fed controls) were allowed to eat *ad-libitum* between 21.00 and 09.00 hr. Groups of food-deprived or full-fed E and O were injected with Cc or V at 09.00 hr (t_0) (n=3/group). Immediately after injections, a pre-weighed chow-filled jar was placed in each cage. At 10.00 hr, jars were removed and weighed; measures of consumed food were adjusted by subtracting the weight of food crumbs on underlying paper [Briski and Nedungadi, 2009]. All animals used in this study exhibited cerebrospinal fluid reflex from the cannula tip on day 12; post-mortem histological examination confirmed accuracy of cannula placements within the CV4.

Western Blot Analysis of AMPK Activity and Neuropeptide Expression in Micropunched Neural Structures

For each animal, PVH, ARH, VMH, and LHA tissues from one hemi-forebrain were collected in microcentrifuge tubes containing 20 μL tissue lysis buffer (2% SDS, 0.05 M DTT, 10% glycerol, 1 mM EDTA, 60 mM Tris-HCl, pH 7.2) for heat denaturation. For each treatment group, tissue aliquots from individual subjects were combined and separated on 10–15% gradient Tris-glycine gels (90 V; 105 min; Tris-glycine SDS running buffer), as described [Cherian and Briski, 2011; 2012]. Proteins were transblotted (30 V; overnight; 4°C; Towbin buffer) to 0.45 μm PVDF-Plus membranes (prod. no. PV4HY00010; Osmonics Inc., Gloucester, MA). After treatment with Western blot signal enhancer (prod. no. 21050; Pierce, Rockford, IL), membranes were blocked (2 hr) with Tris-buffered saline, pH 7.4 (TBS), containing either 0.1 % Tween-20 (prod. no. P9416; Sigma Aldrich, St. Louis, MO) plus 2% bovine serum albumin (prod. no. 81003; MP Biomedicals, Solon, OH; TBS-T-BSA) or 5% normal donkey serum prior to overnight incubation (4°C) with primary antisera. For each hypothalamic structure, proteins of interest were probed with Santa Cruz Biotechnology, Inc. (Santa Cruz, CA) primary polyclonal antisera raised in rabbit against $AMPK_{\alpha 1/2}$ (1:1,000; prod. no. sc-25792) [evaluated in PVH, ARH, VMH, LHA]; $phosphoAMPK_{\alpha 1/2}$ (pAMPK; 1:1,000; prod. no. sc-33524) [evaluated in PVH, ARH, VMH,

LHA]; pro-opiomelanocortin (POMC; 1:500; prod. no. sc-20148) [evaluated in ARH]; neuropeptide Y (NPY; 1:500; prod. no. sc-28943) [evaluated in ARH]; or steroidogenic factor-1 [(SF-1; 1:500; prod. no.sc-2874) [evaluated in VMH], or raised in goat against CRF (1:1,000; prod. no. sc-1759) [evaluated in PVH] or orexin-A (ORX; 1:500; prod. no. sc-8070) [evaluated in LHA], as described [Alenazi et al., 2014]. For each treatment group, pooled cDVC tissue was incubated with antisera against $AMPK_{\alpha 1/2}$, $pAMPK_{\alpha 1/2,}$ or the catecholamine biosynthetic enzyme dopamine-beta-hydroxylase (DβH; 1:500; prod. no. sc-15318, Santa Cruz Biotechnol.) [Ibrahim and Briski, 2014; Ibrahim et al., 2015]. The housekeeping protein α-tubulin was probed with monoclonal antibodies (1:1,000; prod. no. CP06; EMD Millipore, Billerica, MA). Membranes were incubated (1 hr) with peroxidase-conjugated goat anti-mouse (1:5,000; prod. no. NEF822001EA; PerkinElmer, Boston, MA), goat anti-rabbit (1:5,000; prod. no. NEF812001EA; PerkinElmer) or donkey anti-goat (1:5,000; prod. no. sc-2020; Santa Cruz Biotechnol.) secondary antisera. After incubation with Supersignal West Femto Maximum Sensitivity chemiluminescent substrate (prod. no. 34096; ThermoFisherScientific, Inc., Rockford, IL), signals were visualized in a Syngene G: box Chemi. Band optical density (O.D.) was quantified with Genetool 4.01 software (Syngene; Frederick, MD), and expressed relative to α-tubulin. Protein molecular weight markers were included in each Western blot analysis. Immunoblots were performed in triplicate at minimum.

ELISA Analysis of NE Content of Micropunched Structures

Pooled micropunches of the anteroventral periventricular nucleus (AVPV), medial preoptic nucleus (MPN), PVH, ARH, VMH, dorsomedial hypothalamic nucleus (DMH), and LHA from the remaining hemi-forebrain were collected in 100 μL of 0.01 N HCl containing 1 mM EDTA and 4 mM sodium metabisulfite, and homogenized. For each treatment group, tissue aliquots from individual subjects were combined and assayed for NE levels using Noradrenaline Research ELISA kit reagents (prod. no. BA E-5200; Rocky Mountain Diagnostics, Inc., Colorado Springs, CO), per kit instructions [Shrestha et al., 2014]. Briefly, standard (10 uL) and control (10 uL) solutions and sample aliquots (80 uL) were pipetted into individual extraction plate wells, then diluted to 100 uL with distilled water. Plates were sequentially incubated by shaking at 600 rpm with TE buffer (25 μL), acylation buffer (150 μL) plus acylation reagent (25 μL), and hydrochloric acid (100 uL). 90 uL of extracted samples, standards, and controls were transferred to individual microtiter plate wells, mixed with enzyme solution (25 μL), and incubated for 37°C for 2 hr. Sample, standard, and control well aliquots (100 μL) were transferred to pre-coated Noradrenaline Microtiter strip wells, mixed with 50 μL of primary antiserum, then incubated for 15-20 hr at 2-8°C. After plate contents were discarded, wells were washed 4x, then incubated with enzyme conjugate (100 uL) for 30 min. Wells were emptied, washed 4x, then incubated for 20-30 min with 100 μL of substrate. After termination of reactions with 100 μL stop solution, contents absorbance for each well was read at 450 nm in an Emax Precision Microplate Reader (Molecular Devices, LLC, Sunnyvale, CA).

Analysis of Caudal DVC ATP Content

ATP levels were measured using Enliten™ ATP bioluminescence detection kit reagents, per kit instructions (prod. no. FF2000; Promega Corp., Madison, WI). In brief, tissues were

homogenized in 1% trichloroacetic acid (TCA), and centrifuged at 5000 rpm (5 min). Supernantant aliquots (50 μL) were neutralized with 450 μL of Tris-acetate buffer, and pH adjusted to 7.75. After addition of rL/L (luciferase) reagent to unknowns and ATP standards, light intensity (560 nm) was measured with a luminometer and expressed as relative light units (RLU).

Statistical Analyses

Mean food intake, normalized tissue protein O.D., tissue NE, and tissue ATP values were evaluated by two-way ANOVA and Student-Newman-Kuel's *post-hoc* test. Food intake data was evaluated by three-ANOVA and Student-Newman-Kuel's *post-hoc* test. Differences of $p<0.05$ were considered significant.

Results

Figure 1 depicts effects of caudal fourth ventricular (CV4) administration of the AMPK inhibitor Cc on cDVC AMPK and pAMPK protein expression in O- versus E-implanted OVX female rats. AMPK protein levels did not differ between V-injected O and E rats, and were resistant to Cc administration (Figure 1.A). Data in Figure 1.B show that cDVC pAMPK was reduced in E/V versus O/V groups (*$F_{3,12}=53.9$; $p<0.0001$; E effect: $F=33.7$; $p<0.0001$*), and was decreased by Cc in both O and E (*Cc effect: $F=125.9$; $p<0.0001$*). Figure 1.C indicates that cDVC ATP levels were higher in O versus E ratsm and suppressed by Cc in O rats only (*$F_{3,16}=5.09$, $p=0.0115$; E effect: $F=4.53$; $p=0.04$*); *Cc effect:* F=5.83; p=0.02; Cc and E interaction: F=4.91; p=0.04). Data in Figure 2 reveal that cDVC DβH enzyme protein profiles decreased in E/V versus O/V, but augmented by Cc in E rats only. DβH data exhibited significant main ($F_{3,8}=8.85$, $p<0.006$), Cc (F=17.05, $p<0.003$), and Cc and E interaction (F=5.26, $p<0.05$) effects.

Figure 3 shows effects of Cc treatment on PVH AMPK (Figure 3.A), pAMPK (Figure 3.B), and CRH (Figure 3.C) protein levels in O- vs. E-implanted OVX rats. Cc decreased PVH pAMPK in O animals (*$F_{3,12}=6.9463$, $p=0.006$*), and both AMPK (*$F_{3,8}=18.07$; $p=0.0006$; Cc effect: $F=22.02$; $p=0.002$; Cc and E interaction: $F=27.11$; $p=0.001$*) and pAMPK (*Cc effect: $F=20.32$, $p=0.001$*) in E rats. PVH CRH profiles were diminished by Cc in O, but not E (*$F_{3,12}=6.76$; $p=0.006$; Cc effect: $F=16.3$; $p=0.001$*).

Figure 4 depicts Cc-induced patterns of ARH AMPK (Figure 4.A), pAMPK (Figure 4.B), POMC (Figure 4.C), and NPY (Figure 4.D) protein expression in O vs. E rats. Cc did not alter ARH AMPK or pAMPK content. POMC protein profiles were diminished in O/Cc versus O/V and in E/Cc versus E/V ($F_{3,16}=26.9$; $p<0.0001$; Cc effect: F=58.2; p<0.0001); E effect: F=22.1; p=0.0002). ARH NPY content was inhibited or increased by Cc in O and E, respectively ($F_{3,8}=27.5$; p=0.0001; Cc and E interaction: F=76.7; p<0.0001).

Data in Figure 5 show that CV4 administration of Cc altered VMH AMPK (Figure 5.A) and pAMPK (Figure 5.B) profiles in E, but not O. Cc treatment did not alter SF-1 protein expression in O or E compared to V controls. VMH AMPK data analysis revealed significant main (*$F_{3,8}=18.3$; $p=0.001$), Cc ($F=12.7$; $p=0.007$*), E (*$F=13.73$; $p=0.006$*), and Cc

and E interaction *(F=28.5; p=0.001)* effects. VMH pAMPK data showed significant main ($F_{3,12}$=15.3; p=0.0002), Cc (*F=27.3; p=0.0002*) and E (*F=16.0; p=0.001*) effects.

Figure 6 depicts effects of Cc on LHA AMPK (Figure 6.A), pAMPK (Figure 6.B), and ORX-A protein (Figure 6.C) content. Cc inhibited LHA pAMPK expression in E/Cc versus E/V, with significant main ($F_{3,8}$=4.58; p=0.003), Cc (*F=6.68; p=0.03*), and Cc and E interaction (*F=7.24; p=0.027*) effects. Cc administration did not alter LHA ORX-A profiles in E or O animalsw.

Data presented in Figures 7 and 8 describe effects of CV4 administration of Cc on NE content of the AVPV (Figure 7.A), MPN (Figure 7.B), PVH (Figure 7.C), ARH (Figure 7.D), VMH (Figure 8.A), DMH (Figure 8.B), and LHA (Figure 8.C). Results show that Cc treatment augmented NE levels in the AVPV ($F_{3,14}$=7.46; p=0.003), MPN ($F_{3,12}$=10.78; p=0.001), and DMN ($F_{3,9}$=13.6; p=0.001) in E. Meanwhile, the O/Cc group exhibited increased NE activity in the PVH ($F_{3,14}$=4.04; p=0.029) and VMH ($F_{3,13}$=11.4; p=0.001), but decreased ARH ($F_{3,12}$=4.75; p=0.0208) and LHA ($F_{3,11}$=8.17; p=0.004) NE content compared to O/V. Significant E effects were observed for AVPV (*F=6.20; p=0.02*), MPN (*F=7.86; p=0.01*), PVH (*F=5.15; p=0.03*), VMH (*F=7.64; p=0.01*), and LHA (*F=11.3; p=0.006*) data. Significant Cc effects were observed for AVPV (*F=10.6; p=0.005*), MPN (*F=25.6; p=0.0003*), ARH (*F=6.98; p=0.02*), VMH (*F=13.8; p=0.002*), DMH (*F=14.8; p=0.003*), and LHA (*F=8.55; p=0.013*) data. Cc and E interaction effects were observed for ARH (*F=7.013; p=0.02*), VMH (*F=13.4; p=0.002*), and DMH (*F=21.3; p=0.001*) data.

Figure 9 depicts effects of Cc administration on food intake by O versus E rats following 12 hour interruption of feeding. Cc significantly reduced re-feeding by O and E relative to vehicle-injected animals; this treatment completely or incompletely reduced consumption to levels exhibited by full-fed rats in E and O, respectively. Cc also decreased ad-libitum food intake in E, but not O. Data show significant main ($F_{7,20}$=254.9; p<0.0001), 12 hour suspension of feeding (*F=254.9, p<0.0001*), Cc (*F=64.34, p<0.0001*), and interaction [suspended feeding and Cc (*F=13.19, p=0.002*); suspended feeding and E (*F=112.30; p = 0.002*)] effects.

Discussion

This study investigated the premise that estradiol governs innate control of hypothalamic AMPK, metabolic neuropeptide, and NE activity by dorsomedial hindbrain AMPK. Data show that intra-caudal fourth ventricular administration of the AMPK inhibitor Cc suppressed PVH pAMPK expression in both O- and E-implanted OVX animals, and deactivated that sensor in additional hypothalamic loci [VMH; LHA] in the latter group. Pharmacological inhibition of hindbrain AMPK activity elicited divergent changes in PVH CRH and ARH NPY content in OVX+O (↓) versus OVX+E (↔), but suppressed ARH POMC protein profiles in both groups. Cc treatment also elicited site-specific changes in NE activity, as this paradigm either increased [PVH; VMH] or decreased [ARH; LHA] NE in O, but uniformly elevated NE content in other neural structures [AVPV; MPN; DMH] in E. Food intake by Cc-injected E versus O groups was correspondingly completely or partially normalized to full-fed control level, implicating dorsomedial hindbrain AMPK in

physiological stimulus-induced feeding in females. These correlative results suggest that hindbrain sensor-derived input may target common (POMC) as well as distinctive hypothalamic neuropeptide targets (CRH; NPY) in absence versus presence of estrogen. Results moreover imply a role for estradiol in the distribution of hypothalamic AMPK controlled by hindbrain AMPK activity state. Importantly, corresponding outcomes point to NE as a likely effector of dorsomedial hindbrain AMPK deactivation on the hypothalamus, and show that location and direction of Cc-induced change in hindbrain sensor-driven NE activity are controlled by E. Current evidence for site-specific changes in NE levels in O/Cc animals supports the novel concept that sensor-driven noradrenergic input to the hypothalamus is bi-directional when estrogen is lacking.

AMPK levels in the cDVC were equivalent, whereas pAMPK expression was elevated in OVX+O versus OVX+E rats, results that demonstrate greater sensor activity in the former. AMPK activation is regulated in part by intracellular AMP/ATP ratio. Evidence for parallel pAMPK and ATP augmentation in O- versus E-implanted rats implies that cDVC AMP may be disproportionately increased when estradiol is lacking, thereby amplifying deviation of AMP relative to ATP and thus promoting AMPK activation. Alternatively, whole-cDVC measurements in O rats that demonstrate a net increase in ATP content may obscure local reductions in ATP in distinct cell populations, including cells that express AMPK. This work underscores the need for high-resolution analytical techniques for cellular-level ATP quantification in order that the role of estradiol in cell type-specific ATP responses to metabolic stressors, including metabolo-sensory versus non-metabolic-sensing cells, can be investigated. Current data show that Cc treatment inhibited pAMPK profiles in cDVC of OVX+O and OVX+E rats, and either decreased or did not modify tissue ATP content, respectively, in that structure. Since ATP in the O/Cc group was reduced to levels measured in both vehicle- and Cc-treated E rats, we speculate that estradiol-mediated reductions in cDVC ATP may approximate minimal thresholds for normal cell function and thus constrain further decrements in ATP content despite diminution of signals of energy deficiency.

The present studies implicate estradiol in regulation of hypothalamic AMPK sensitivity to inherent hindbrain AMPK activation. More hypothalamic loci exhibited diminished pAMPK expression in OVX+E [PVH, VMH; LHA] versus OVX+O [PVH] in response to intra-CV4 Cc delivery, suggesting that estrogen may enhance hypothalamic sensor reactivity to and/or strength of hindbrain sensor-mediated input to those structures. Metabolo-sensory A2 noradrenergic neurons are a likely caudal hindbrain substrate for estrogenic control of hindbrain-hypothalamic AMPK connectivity, as these cells exhibit steroid-dependent adjustments in Fos expression in response to CV4 AICAR administration to OVX rats [Ibrahim et al., 2013] and are critical for hypoglycemia-associated increases in hypothalamic astrocyte AMPK activity in OVX+E animals [Tamrakar and Briski, 2015]. The latter work emphasizes the additional need to characterize the hypothalamic cell compartments (e.g. neurons, astrocytes, etc.) that express hindbrain-sensitive AMPK. Previous studies investigating pharmacological augmentation of dorsomedial hindbrain AMPK activity documented CV4 AICAR stimulation of PVH pAMPK levels in E, but not O [Alenazi et al., 2014], while the current work demonstrates inhibitory effects of Cc on PVH pAMPK profiles in both E and O. These results imply that estradiol may permit intensification of pAMPK expression beyond baseline in response to superimposed energy deficit simulated

by AICAR. Earlier work also illustrates AICAR-induced suppression of VMH pAMPK profiles in O and E, while Cc treatment here also inhibited VMH pAMPK expression in E. Similar effects of AICAR and Cc in the presence of estradiol support the possibility that this hormone may diminish VMH pAMPK levels (perhaps involving different neurotransmitter neuron populations) in response to incremental or decremental shifts in hindbrain sensor activity.

Western blot measures of metabolic neuropeptide content of hypothalamic structures characterized by Cc-induced reductions in AMPK activity in E animals showed PVH CRH, VMH SF-1, and LHA ORX-A profiles to be refractory to hindbrain AMPK deactivation. One possible explanation of these data is that hindbrain AMPK lacks functional connectivity with these neurotransmitters; alternatively, a lack of change in neurotransmitter levels may mask parallel adjustments in peptide synthesis and anterograde axonal transport away from the cell body. This outcome underscores the need for continuing efforts to identify other orexigenic and anorexigenic neurotransmitters synthesized in these and other hypothalamic loci that are inhibited or increased, respectively, by CV4 Cc injection to OVX + E rats, and to assess the role of those hindbrain AMPK-sensitive neurochemicals in Cc-mediated suppression of feeding in those animals. Moreover, it would be informative to learn if hindbrain sensor-controlled AMPK activity in the PVH, VMH, and LHA of OVX + E animals exerts local effects, e.g. on cellular energy metabolism, and/or governs regulatory signaling in pathways that mediate systemic activities. Although Cc did not modify ARH pAMPK expression in E or O animals, E/Cc and O/Cc groups exhibited decreased POMC protein expression. POMC is a precursor peptide that yields several bioactive neurotransmitters upon cleavage, including peptides that inhibit (α-melanocortin) or stimulate (β-endorphin) food intake. In the present context, diminished yield of β-endorphin may play a role in Cc-associated suppression of feeding in both groups. There remains a critical need to determine if hindbrain AMPK activation regulates post-translational POMC processing, including mechanisms that control absolute abundance and relative proportions of β-endorphin versus α-melanocortin. Cc administration elicited opposite adjustments in ARH NPY profiles in O/Cc versus E/Cc as neuropeptide levels were correspondingly suppressed or elevated in those groups. In the ARH, AMPK is localized to both NPY and POMC neurons [Cai et al., 2007; Claret et al., 2007; Mountjoy et al., 2007; Andrews et al., 2008; Gujar et al., 2014]. It would be insightful to learn if Cc-induced decline in NPY in O rats involves direct or indirect mechanisms of AMPK action and is involved in treatment-associated inhibition of food intake.

Outcomes of ELISA analysis of hypothalamic NE content show that noradrenergic tone driven by dorsomedial hindbrain AMPK activity is site-specific, results that challenge the conventional assumption of uniformity of noradrenergic signals conveying hindbrain metabolic information to hypothalamic targets. Hindbrain Cc administration caused contradictory [↑: PVH, VMH; ↓: ARH, LHA] changes in NE levels in OVX+O, implying that innate dorsomedial AMPK activity simultaneously inhibits or promotes NE accumulation in those sites. It is intriguing to speculate whether AMPK-sensitive NE projections to these two distinctive sets of loci derive from separate populations of A2 neurons, or if sensor activity elicits opposite changes in neurotransmitter content along axon branches diverging to innervate the PVH/VMH versus ARH/LHA. It is recognized that

analysis of steady-state NE tissue content does not permit definitive insight on how hindbrain AMPK deactivation impacts the ratio of NE synthesis/metabolism/release within individual hypothalamic structures. Implementation of experimental protocols such as pharmacological manipulation of catecholamine synthesis or degradation would clarify Cc treatment effects on local NE release and synthesis, respectively. Despite bi-directional changes in hypothalamic NE content in Cc-treated O rats, these animals show no coincident change in net cDVC DβH enzyme protein. One possibility is that cDVC-wide analysis of this protein profile may obscure opposite adjustments in expression in subpopulations of AMPK-expressing A2 neurons. Alternatively, DβH expression may be refractory to Cc in the absence of estradiol. In this scenario, sensor deactivation may increase [PVH;VMH] or decrease [ARH;LHA] NE accumulation through effects on NE degradation and/or release in the absence of altered synthesis rate. Augmented NE tissue content could thus reflect Cc-induced decreases in NE breakdown or release, whereas decreases in NE could indicate treatment augmentation of metabolism and/or release. Ongoing research seeks to determine local targets and functional effects of dorsomedial hindbrain AMPK-guided noradrenergic input. It would be of interest to learn if increased NE input to the OVX+O PVH stimulates pAMPK and CRH expression, or if augmented NE tone in the ARH elevates POMC protein profiles in those animals.

On the other hand, Cc augmentation of AVPV, MPN, and DMH NE levels in OVX+E implies that in an estrogen-positive state dorsomedial hindbrain AMPK activation is inversely correlated with NE content of a wholly different set of forebrain structures. These data show that estradiol determines hypothalamic targets of NE signaling of hindbrain sensor status; molecular mechanisms involved in respective hormonal ‘silencing’ and ‘un-silencing’ of AMPK-sensitive noradrenergic projections to the PVH, etc. versus preoptic loci and DMH remain to be elucidated. Evidence here for hindbrain AMPK-dependent NE input to the AVPV and MPN, structures of critical relevance to reproduction, is consistent with recent reports that steroid positive-feedback activation of the gonadotropin-releasing hormone-pituitary luteinizing hormone neuroendocrine axis is restrained by metabolic inhibition of A2 nerve cell noradrenergic signaling [Ibrahim and Briski, 2014]. The related premise that estrogen inhibits dorsomedial hindbrain AMPK-driven noradrenergic transmission is bolstered by increased cDVC DβH enzyme protein in Cc-treated E rats, findings that imply that in the presence of estradiol sensor activation elicits unambiguous suppression of DVC NE signals. Data showing Cc augmentation of DβH suggest that coincident reductions in NE content in the AVPV, MPN, and DMH likely reflect diminished synthesis. Along the same lines, the lack of change in NE levels in other hypothalamic loci may indicate an equivalent increase in release rate, thereby sustaining net tissue NE content.

CV4 Cc administration significantly reduced feeding in both O and E rats after a 12 hour period of suspended food intake, results that implicate dorsomedial hindbrain AMPK in neural mechanisms controlling physiological stimulus-induced feeding in females. In E animals, this treatment paradigm normalized re-feeding to full-fed ad-libitum levels, suggesting that estradiol likely allows primary if not exclusive impetus to eat to emanate from this sensor. Observations of partial suppression of re-feeding by Cc administration to O rats imply that in an estrogen-negative state, dorsomedial hindbrain AMPK along with other as-yet-unidentified sensory entities regulate compensatory consumption following brief

interruption of food intake. The current data reveal a trend for decreased food intake by E/V versus O/V animals that was statistically insignificant, whereas previous work involving larger-sized treatment groups showed significant less consumption by E- versus O-implanted OVX rats over the first hour of re-feeding after 12 hours of food deprivation [Ibrahim and Briski, 2014]. Cc administration to adult male rats by a similar delivery route diminished ad-libitum eating [Hayes et al., 2009] and 2-deoxy-glucose – induced hyperphagia [Li et al., 2011]. The present data show that Cc decreased feeding by full-fed E, but not O rats is reduced by Cc; further research is needed to determine if estradiol, a metabolite of testosterone, is crucial for hindbrain AMPK regulation of consumption by full-fed males. Cc treatment did not inhibit re-feeding by male rats after two hours of suspended intake [Li et al., 2011], suggesting that phagic responses to varying intervals of intermittent feeding intake may be controlled by AMPK sensors located in different brain sites or that short-term cessation may evoke AMPK-independent mechanisms.

In summary, correlative results of current studies support a role for estradiol in regulation of hindbrain-hypothalamic AMPK connectivity in the female rat. Excluding POMC, hypothalamic neurotransmitter targets of dorsomedial hindbrain AMPK may differ in presence vs. absence of estradiol. Moreover, estradiol may establish hypothalamic targets of hindbrain AMPK-driven NE signaling. Pharmacological antagonism of hindbrain AMPK augmented [PVH; VMH] or reduced [ARH; LHA] NE accumulation in OVX+O animals, demonstrating sensor-induced bimodal noradrenergic signaling to those structures, but uniformly elevated NE content in other neural structures [AVPV; MPN; DMH] in OVX+E. Lastly, differences in extent of Cc-mediated inhibition of food intake in E versus O animals suggest that estradiol may determine the origin of stimuli that control physiological patterns of feeding in females.

References

Alenazi FSH, Ibrahim BA, Briski KP. Estradiol regulates effects of hindbrain AICAR administration on hypothalamic AMPK activity and metabolic neurotransmitter mRNA and protein expression. J. Neurosci. Res. 2014; 93:651–659. [PubMed: 25476093]

Andrews ZB, Liu ZW, Wallingford N, Erion DM, Borok E, Friedman JM, Tschöp MH, Shanabrough M, Cline G, Shulman GI, Coppola A, Gao XB, Horvath TL, Diano S. UCP2 mediates ghrelin's action on NPY/AgRP neurons by lowering free radicals. Nature. 2008; 454:846–851. [PubMed: 18668043]

Briski KP, Marshall ES, Sylvester PW. Effects of estradiol on glucoprivic transactivation of catecholaminergic neurons in the female rat caudal brainstem. Neuroendocrinology. 2001; 73:369–377. [PubMed: 11408778]

Briski KP, Nedungadi TP. Adaptation of feeding and counter-regulatory hormone responses to intermediate insulin-induced hypoglycaemia in the ovariectomised female rat: effects of oestradiol. J. Neuroendocrinol. 2009; 21:578–585. [PubMed: 19500228]

Butcher RL, Collins WE, Fugo NW. Plasma concentrations of LH, FSH, progesterone, and estradiol-17beta throughout the 4-day estrous cycle of the rat. Endocrinology. 1974; 94:1704–1708. [PubMed: 4857496]

Cai F, Gyulkhandanyan AV, Wheeler MB, Belsham DD. Glucose regulates AMP ctivated protein kinase activity and gene expression in clonal, hypothalamic neurons expressing proopiomelanocortin: additive effects of leptin or insulin. J Endocrinol. 2007; 192:605–614. [PubMed: 17332528]

Cherian A, Briski KP. Quantitative RT PCR and immunoblot analyses reveal acclimated A2 noradrenergic neuron substrate fuel transporter, glucokinase, phospho-AMPK, and dopamine-beta-hydroxylase responses to hypoglycemia. J. Neurosci. Res. 2011; 89:1114–1124. [PubMed: 21488089]

Cherian A, Briski KP. A2 noradrenergic nerve cell metabolic transducer and nutrient transporter adaptation to hypoglycemia: Impact of estrogen. J. Neurosci. Res. 2012; 90:1347–1358. [PubMed: 22431334]

Claret M, Smith MA, Batterham RL, Selman C, Choudhury AI, Fryer LG, Clements M, Al-Qassab H, Heffron H, Xu AW, Speakman JR, Barsh GS, Viollet B, Vaulont S, Ashford ML, Carling D, Withers DJ. AMPK is essential for energy homeostasis regulation and glucose sensing by POMC and AgRP neurons. J Clin Invest. 2007; 117:2325–2336. [PubMed: 17671657]

Goodman RL. A quantitative analysis of the physiological role of estradiol and progesterone in the control of tonic and surge secretion of luteinizing hormone in the rat. Endocrinology. 1978; 102:142–150. [PubMed: 570477]

Gujar AD, Ibrahim BA, Tamrakar P, Koshy Cherian A, Briski KP. Hindbrain lactostasis regulates hypothalamic AMPK activity and hypothalamic metabolic neurotransmitter mRNA and protein responses to hypoglycemia. Amer. J. Physiol. Regul. Integ. Comp. Physiol. 2014; 306:R457–R469.

Hardie DG. Minireview: The AMP-activated protein kinase cascade: the key sensor of cellular energy status. Endocrinology. 2003; 144:5179–5183. [PubMed: 12960015]

Hayes MR, Skibicka KP, Bence KK, Grill HJ. Dorsal hindbrain 5'-adenosine monophosphate-activated protein kinase as an intracellular mediator of energy balance. Endocrinology. 2009; 150:2175–2182. [PubMed: 19116341]

Ibrahim BA, Alenazi FSH, Briski KP. Energy status determines hindbrain signal transduction pathway transcriptional reactivity to AMPK in the estradiol-treated ovariectomized female rat. Neuroscience. 2015; 284:888–899. [PubMed: 25446360]

Ibrahim BA, Briski KP. Role of dorsal vagal complex A2 noradrenergic neurons in hindbrain glucoprivic inhibition of the luteinizing hormone surge in the steroid-primed ovariectomized female rat: Effects of 5-thioglucose on A2 functional biomarker and AMPK activity. Neuroscience. 2014; 269:199–214. [PubMed: 24631866]

Ibrahim BA, Briski KP. Deferred feeding and body weight responses to short-term interruption of fuel acquisition: Impact of estradiol. Horm. Metab. Res. 2015; 47:611–621. [PubMed: 25230326]

Ibrahim BA, Tamrakar P, Gujar AD, Koshy Cherian A, Briski KP. Caudal fourth ventricular administration of the AMPK activator 5-aminoimiazole-4-carboxamide-riboside regulates glucose and counterregulatory hormone profiles, dorsal vagal complex metabolosensory neuron function, and hypothalamic Fos expression. J. Neurosci. Res. 2013; 91:1226–1238. [PubMed: 23825033]

Kale AY, Paranjape SA, Briski KP. I.c.v. administration of the nonsteroidal glucocorticoid receptor antagonist, CP4-72555, prevents exacerbated hypoglycemia during repeated insulin administration. Neuroscience. 2006; 140:555–565. [PubMed: 16626867]

Kahn BB, Alquier T, Carling D, Hardie DG. AMP-activated protein kinase: ancient energy gauge provides clues to modern understanding of metabolism. Cell Metabolism. 2005; 1:15–25. [PubMed: 16054041]

Li AJ, Wang Q, Ritter S. Participation of hindbrain AMP-activated protein kinase in glucoprivic feeding. Diabetes. 2011; 60:436–442. [PubMed: 21270255]

Mountjoy PD, Bailey SJ, Rutter GA. Inhibition by glucose or leptin of hypothalamic neurons expressing neuropeptide Y requires changes in AMP-activated protein kinase activity. Diabetologia. 2007; 50:168–177. [PubMed: 17093945]

Shrestha PK, Tamrakar P, Ibrahim BA, Briski KP. Hindbrain medulla catecholamine cell group involvement in lactate-sensitive hypoglycemia-associated patterns of hypothalamic norepinephrine and epinephrine activity. Neuroscience. 2014; 278:20–30. [PubMed: 25084049]

Tamrakar P, Briski KP. Estradiol regulates hypothalamic astrocyte adenosine 5'-monophosphate-activated protein kinase activation by hypoglycemia: role of hindbrain catecholamine signaling. Brain Res. Bull. 2015; 110:47–53. [PubMed: 25497905]

Tamrakar P, Ibrahim BA, Gujar AK, Briski KP. Estrogen regulates energy metabolic pathway and upstream AMPK kinase and phosphatase enzyme expression in dorsal vagal complex metabolosensory neurons during glucostasis and hypoglycemia. J. Neurosci. Res. 2015; 93:321–332. [PubMed: 25231731]

Thammacharoen S, Lutz TA, Geary N, Asarian L. Hindbrain administration of estradiol inhibits feeding and activates estrogen receptor-alpha-expressing cells in the nucleus tractus solitaries of ovariectomized rats. Endocrinology. 2008; 149:1609–1617. [PubMed: 18096668]

Wade GN, Schneider JE. Metabolic fuels and reproduction in female mammals. Neurosci. Biobehav. Res. 1992; 16:235–272.

Highlights

- Compound C (*Cc*) was injected to estradiol or oil implanted ovariectomized rat hindbrain
- *Cc* inhibits hindbrain adenosine 5’-monophosphate-activated protein kinase (AMPK)
- Estradiol regulates hindbrain *Cc* effects on hypothalamic AMPK
- Estradiol determines hypothalamic targets of *Cc*-altered norepinephrine signaling
- *Cc* completely or partially represses feeding in presence versus absence of estradiol

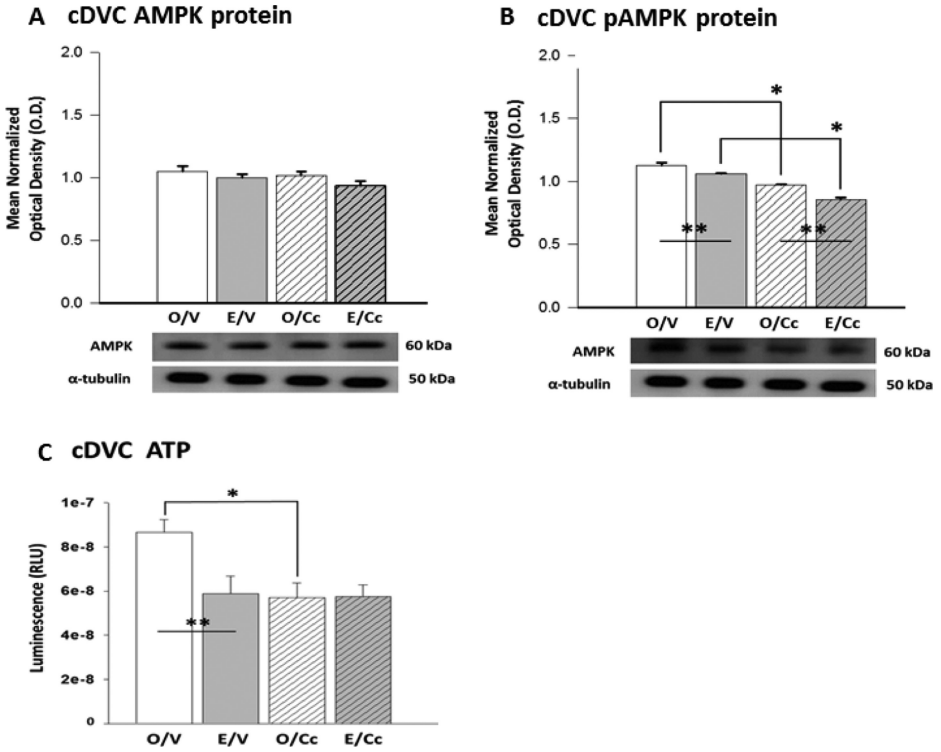

Figure 1. Effects of Caudal Fourth Ventricular (CV4) Administration of the Adenosine 5'-Monophosphate-Activated Protein Kinase (AMPK) Inhibitor, Compound C (Cc), on Hindbrain Caudal Dorsal Vagal Complex (cDVC) AMPK and phosphoAMPK (pAMPK) Levels in Estradiol (E)- and Oil (O)-Implanted Ovariectomized (OVX) Female Rats

Groups of E and O animals were sacrificed 1 hr after Cc administration (n=5 O/Cc, n=5 E/Cc) or V (n=5 O/V, n=5 E/V). Bars in Figures 1.A and 1.B depict mean corresponding normalized cDVC AMPK and pAMPK protein optical density (O.D.) measures ± S.E.M. for O/V [solid white bar], E/V [solid grey bar], O/Cc [diagonal-striped white bar], and E/Cc [diagonal-striped gray bar] treatment groups. Representative immunoblots of AMPK, pAMPK, and the housekeeping protein α-tubulin are shown below respective graphs. cDVC pAMPK data analysis revealed significant main ($F_{3,12}$=53.9; p<0.0001), Cc (F=125.9; p<0.0001), and E (F=33.7; p<0.0001) effects. Bars in Figure 1.C illustrate effects of Cc treatment on E versus O rat cDVC ATP content. cDVC ATP data showed a significant main effect ($F_{3,16}$=5.09, p=0.0115), Cc (F=5.83; p=0.02) and E (F=4.53; p=0.04) effects, and Cc and E interaction (F=4.91; p=0.04). *p <0.05, Cc versus V; **p <0.05, E/V versus O/V.

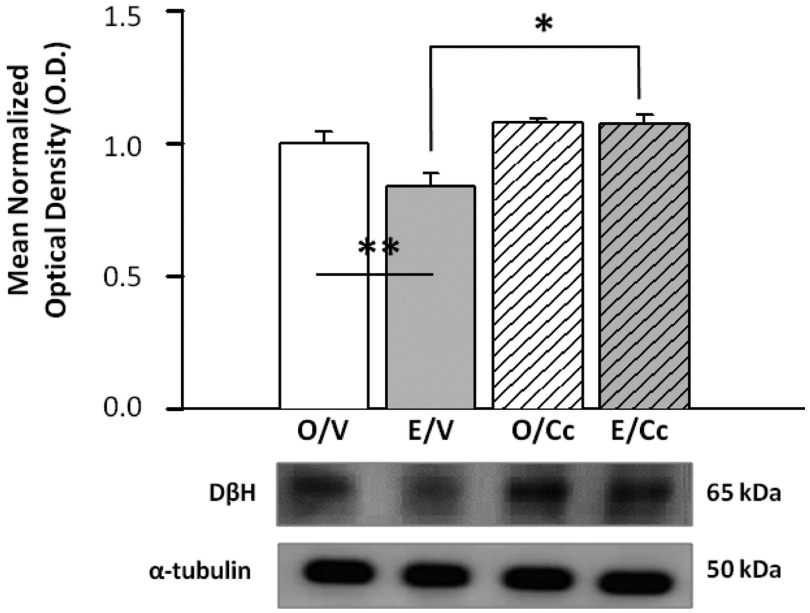

Figure 2. Effects of Cc Treatment on cDVC Dopamine-beta-hydroxylase (DβH) Protein Expression in OVX+E versus OVX+O rats

DβH Western blot analysis was performed on cDVC tissue obtained by micropunch-dissection following Cc administration into the CV4. Bars represent mean normalized DβH protein O.D. measures ± S.E.M. for O/V [solid white bar], E/V [solid grey bar], O/Cc [diagonal-striped white bar], and E/Cc [diagonal-striped gray bar] treatment groups. Typical DβH and α-tubulin Western blots are presented below the graph. DβH data analysis showed significant main ($F_{3,8}$=8.85, p<0.006), Cc (F=17.05, p<0.003), and Cc and E interaction (F=5.26, p<0.05) effects. *p <0.05, Cc versus V; **p <0.05, E/V versus O/V.

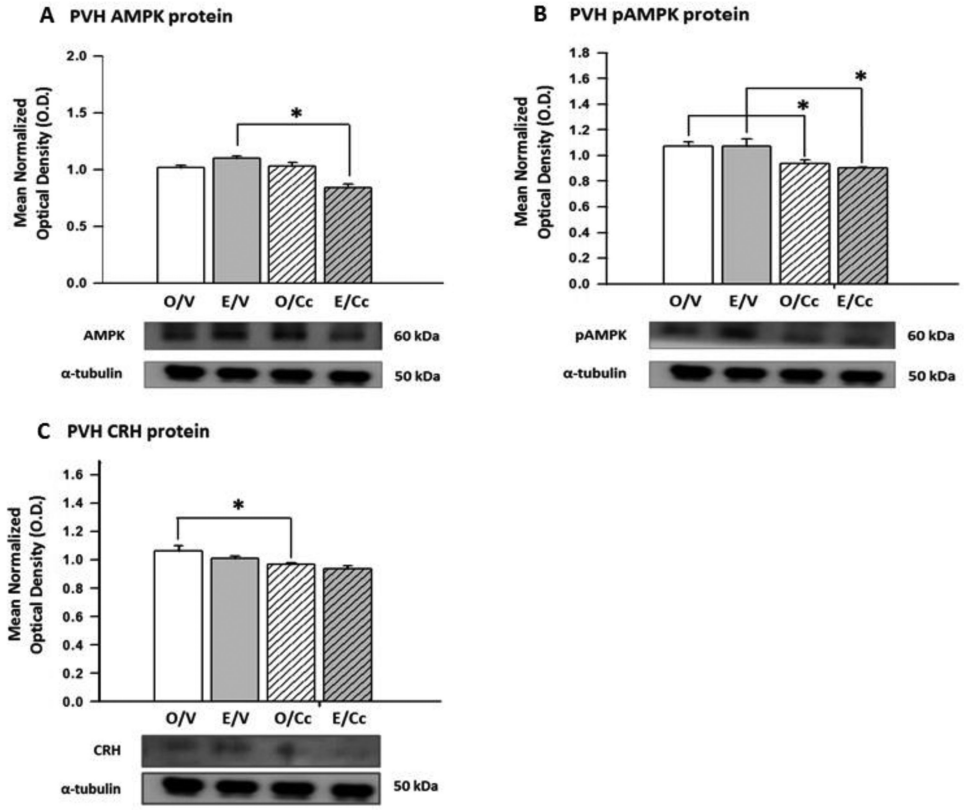

Figure 3. Effects of Intra-CV4 Cc Treatment on Paraventricular Hypothalamic Nucleus (PVH) AMPK, pAMPK, and Corticotropin-Releasing Hormone (CRH) Protein Expression in E- versus O-Implanted OVX Female Rats

Groups of E and O animals were sacrificed at +1 hr after Cc (n=5 O/Cc, n=5 E/Cc) or V (n=5 O/V, n=5 E/V). Data depict mean normalized PVH AMPK (Figure 3.A), pAMPK (Figure 3.B), and CRH (Figure 3.C) protein optical density (O.D.) measures ± S.E.M. for O/V [solid white bar], E/V [solid grey bar], O/Cc [diagonal-striped white bar], and E/Cc [diagonal-striped gray bar] treatment groups. Characteristic neuropeptide and α-tubulin immunoblots are shown below each graph. PVH AMPK data analysis showed significant main ($F_{3,8}$=18.07; p=0.0006) and Cc (F=22.02; p=0.002) effects, and significant Cc and E interaction (F=27.11; p=0.001). For PVH pAMPK, there were significant main ($F_{3,12}$=6.9463, p=0.006) and Cc (F=20.32, p=0.001) effects. For PVH CRH protein, there were significant group ($F_{3,12}$=6.76; p=0.006) and Cc (F=16.3; p=0.001) effects. *p <0.05, Cc versus V.

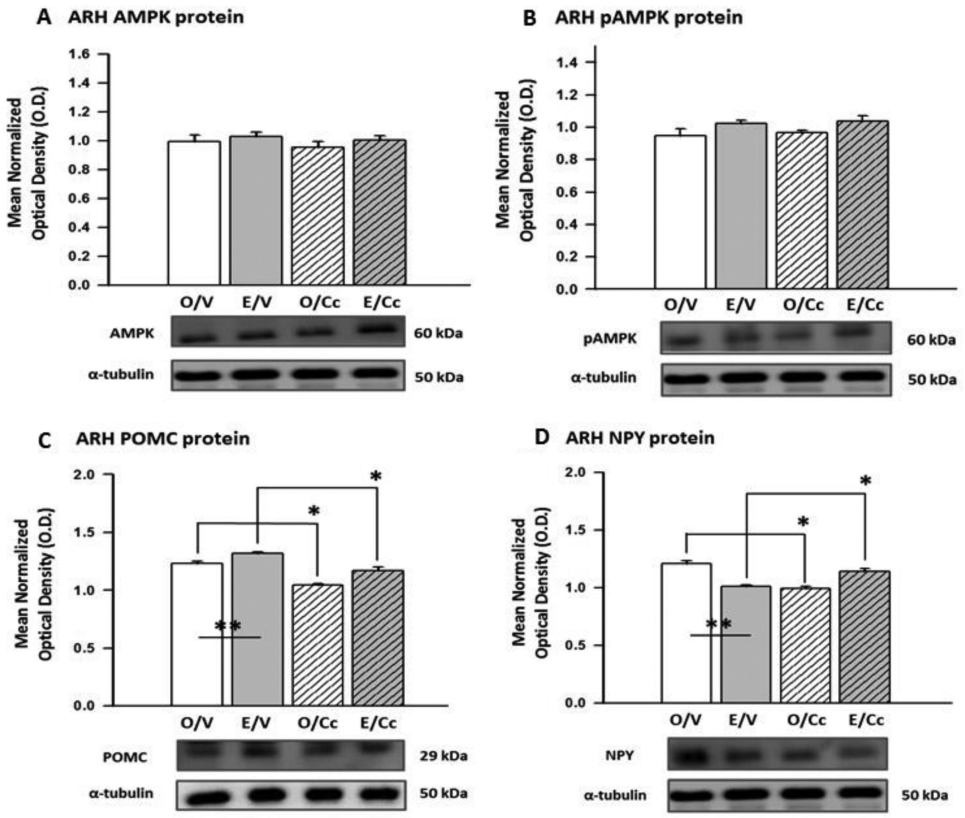

Figure 4. Effects of E on Arcuate Hypothalamic Nucleus (ARH) AMPK, pAMPK, Pro-opiomelanocortin (POMC), and Neuropeptide Y (NPY) Protein Responses to CV4 Cc Treatment of OVX Female Rats

ARH tissue was micropunch-dissected 1 hr after intra-CV4 Cc administration to measure AMPK (Figure 4.A), pAMPK (Figure 4.B), POMC (Figure 4.C), and NPY (Figure 4.D) levels by Western blot analysis. Graphs depict mean normalized protein O.D. measures ± S.E.M. for O/V [solid white bar], E/V [solid grey bar], O/Cc [diagonal-striped white bar], and E/Cc [diagonal-striped gray bar] treatment groups. Typical neuropeptide and α-tubulin Western blots are included in each figure. Analysis of ARH POMC protein data showed significant main ($F_{3,16}$=26.9; p<0.0001), Cc (F=58.2; p<0.0001), and E (F=22.1; p=0.0002) effects. For ARH NPY protein, there was a significant main effect ($F_{3,8}$=27.5; p=0.0001) and significant Cc and E interaction (F=76.7; p<0.0001). *p <0.05, Cc versus V; **p <0.05, E/V versus O/V.

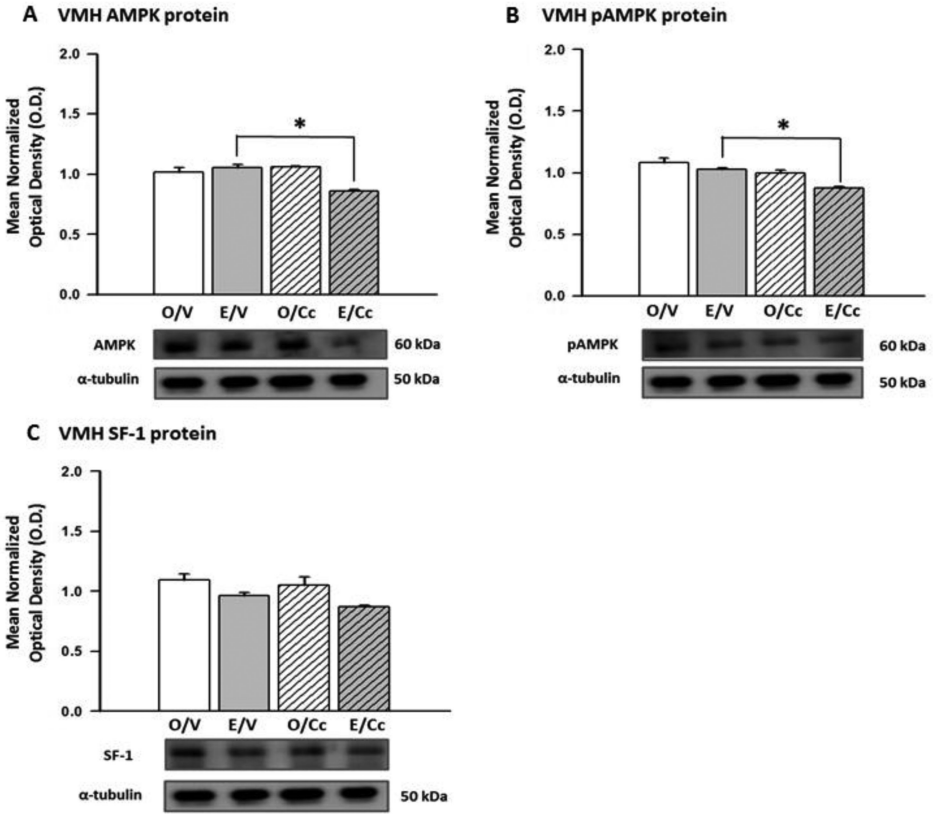

Figure 5. Effects of Intra-CV4 Cc Administration on Ventromedial Hypothalamic Nucleus (VMH) AMPK, phosphoAMPK (pAMPK), and Steroidogenic Factor-1 (SF-1) Protein Expression in OVX+E versus OVX+O Female Rats

Groups of E and O animals were sacrificed 1 hr after treatment with Cc or V. Data depict mean normalized VMH AMPK (Figure 5.A), pAMPK (Figure 5.B), and SF-1 (Figure 5.C) protein O.D. measures ± S.E.M. for O/V [solid white bar], E/V [solid grey bar], O/Cc [diagonal-striped white bar], and E/Cc [diagonal-striped gray bar] treatment groups. Representative neuropeptide and α-tubulin immunoblots are shown below each graph. Statistical analysis of VMH AMPK protein revealed a significant main ($F_{3,8}$=18.3; p=0.001), Cc (F=12.7; p=0.007), and E (F=13.73; p=0.006) effects, and Cc and E interaction (F=28.5; p=0.001). For VMH pAMPK protein, there were significant main ($F_{3,12}$=15.3; p=0.0002), Cc (F=27.3; p=0.0002) and E (F=16.0; p=0.001) effects. *p <0.05, Cc versus V.

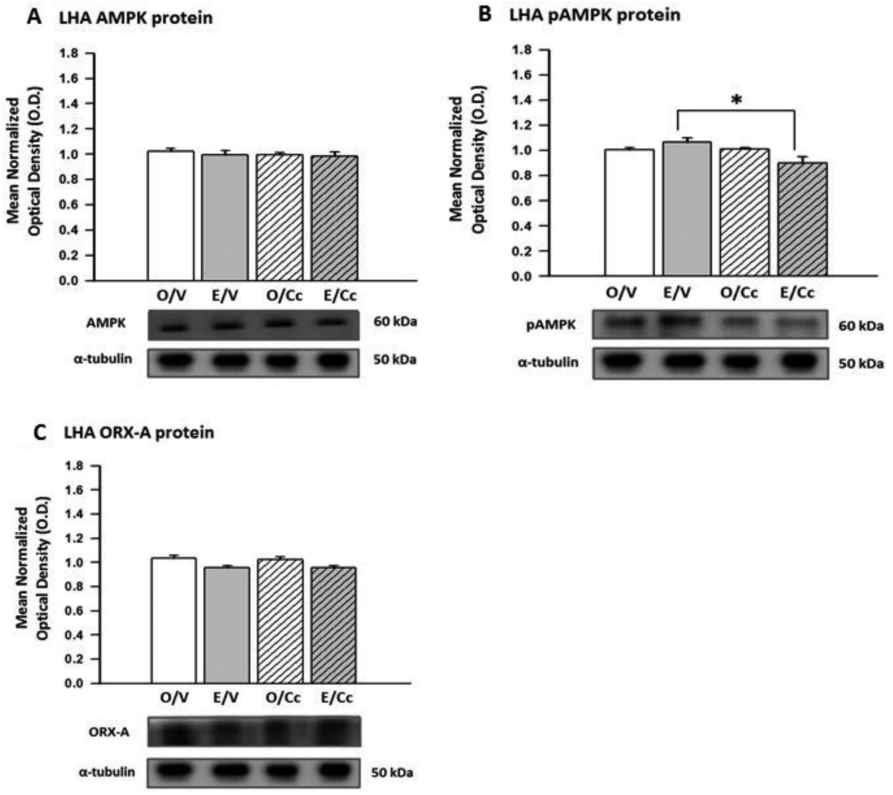

Figure 6. Effects of E on Lateral Hypothalamic Area (LHA) AMPK, pAMPK, and Orexin-A ORX-A Protein Responses to CV4 Cc Treatment of OVX Female Rats

LHA tissue was micropunched 1 hr after intra-CV4 Cc delivery for determination of AMPK (Figure 6.A), pAMPK (Figure 6.B), and ORX-A (Figure 6.C) content by Western blot analysis. Graphs depict mean normalized protein O.D. measures ± S.E.M. for O/V [solid white bar], E/V [solid grey bar], O/Cc [diagonal-striped white bar], and E/Cc [diagonal-striped gray bar] treatment groups. Typical neuropeptide and α-tubulin Western blots are included in each figure. For LHA pAMPK protein, there were significant main ($F_{3,8}$=4.58; p=0.003), Cc (F=6.68; p=0.03), and Cc and E interaction effects (F=7.24; p=0.027). *p <0.05, Cc versus V.

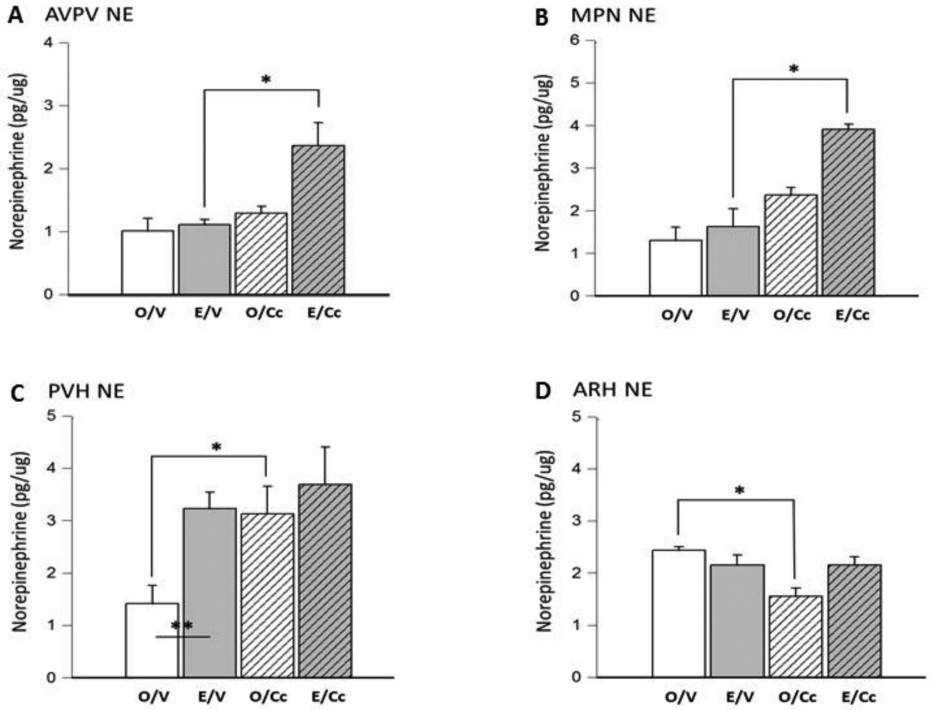

Figure 7. Effects of CV4 Cc Administration on Anteroventral Periventricular Nucleus (AVPV), Medial Preoptic Nucleus (MPN), PVH, and ARH Norepinephrine (NE) Content in E- versus O-Implanted OVX Female Rats

Bars depict mean NE content ± S.E.M. (n=5 rats/group) of pooled AVPV (Figure 7.A), MPN (Figure 7.B), PVH (Figure 7.C), and ARH (Figure 7.D) tissue from V- [O/V, solid white bar; E/V, solid grey bar] or Cc- [O/Cc, diagonal-striped white bar; E/Cc, diagonal-striped gray bar] treated rats. Statistical analysis of AVPV NE data revealed significant main ($F_{3,14}$=7.46; p=0.003), Cc (F=10.6; p=0.005), and E (F=6.20; p=0.02) effects. For MPN NE data, there were significant main ($F_{3,12}$=10.78; p=0.001) and Cc (F=25.6; p=0.0003), and E (F=7.86; p=0.01) effects. PVH NE data analysis showed significant main ($F_{3,14}$=4.04; p=0.029) and E (F=5.15; p=0.03) effects. For ARH NE data, there were significant main ($F_{3,12}$=4.75; p=0.0208) and Cc (F=6.98; p=0.02) effects, and Cc and E interaction (F=7.013; p=0.02). *p<0.05, Cc versus V; **p<0.05, E/V versus O/V.

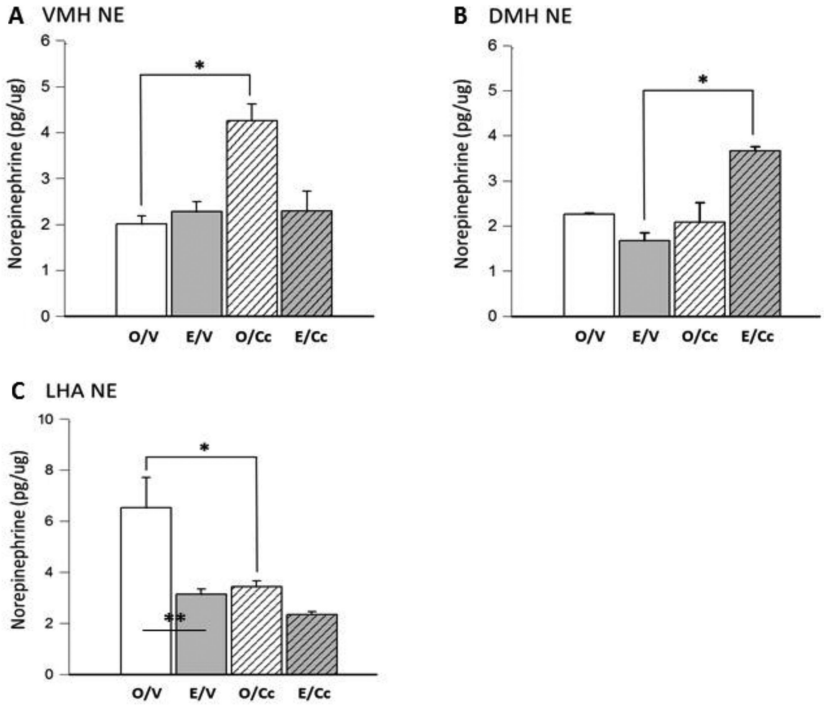

Figure 8. Effects of CV4 Cc Administration on Dorsomedial Hypothalamic Nucleus (DMH), VMH, and LHA NE Content in OVX+E versus OVX+O Female Rats

Bars depict mean NE content ± S.E.M. (n=5 rats/group) of pooled VMH (Figure 8.A), DMH (Figure 8.B, and LHA (8.C) tissue from O/V [solid white bar], E/V [solid grey bar], O/Cc [diagonal-striped white bar], or E/Cc [diagonal-striped gray bar] animals. Statistical analysis of VMH NE data revealed significant main ($F_{3,13}$=11.4; p=0.001), Cc (F=13.8; p=0.002), E (F=7.64; p=0.01), and Cc and E interaction effects (F=13.4; p=0.002). For DMH NE data, there were significant main ($F_{3,9}$=13.6; p=0.001), Cc (F=14.8; p=0.003), and Cc and E interaction effects (F=21.3; p=0.001). For LH NE, there were significant main ($F_{3,11}$=8.17; p=0.004), Cc (F=8.55; p=0.013), and E (F=11.3; p=0.006) effects. *p<0.05, Cc versus V.

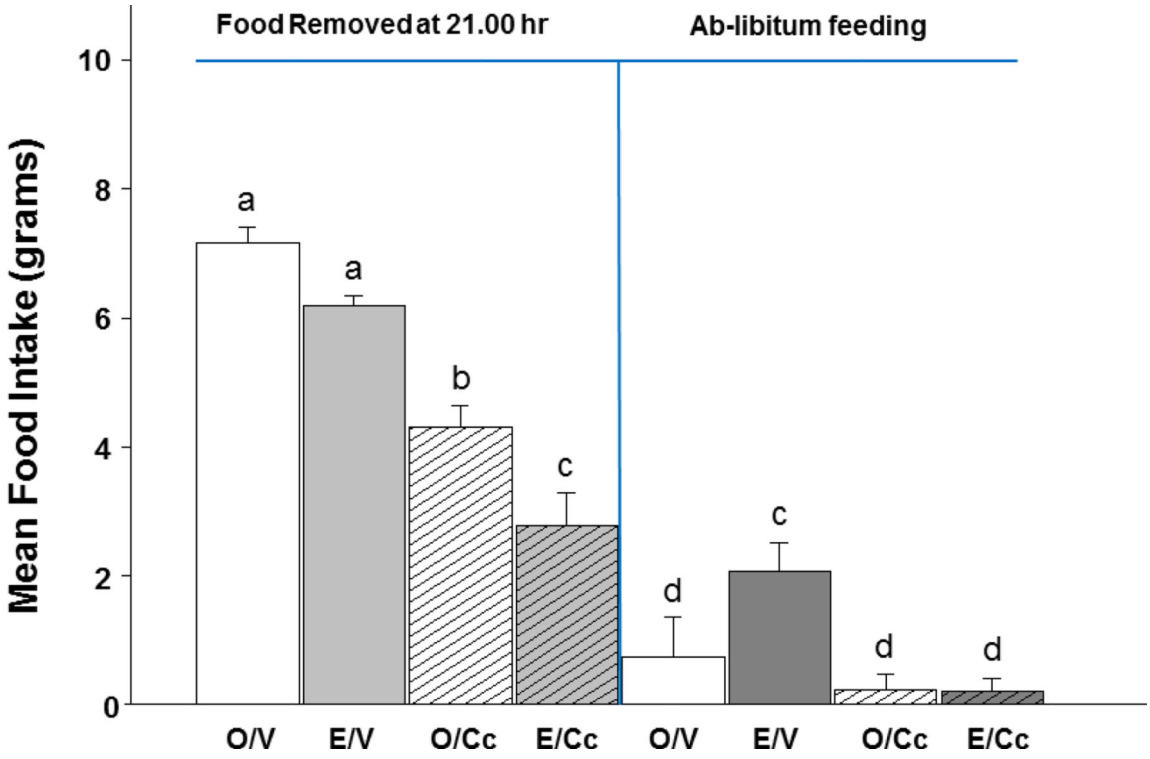

Figure 9. Effects of CV4 Cc Administration on Food Intake in E- versus O-Implanted OVX Female Rats

Groups of OVX+O and OVX+E animals were either food-deprived from 21.00 to 0.900 hr or allowed to eat *ad-libitum* over the same interval. Immediately prior to re-introduction of food at 09.00 hr, rats were injected into the CV4 with Cc (5.0 μg) or vehicle (V). Food intake was measured between 09.00 and 10.00 hr. Bars depict mean food consumed ± S.E.M. by O/V [solid white bar]; E/V [solid grey bar]; O/Cc [diagonal-striped white bar]; and E/Cc [diagonal-striped gray bar] groups of animals after food deprivation [bars 1-4] or *ad-libitum* feeding [bars 5-8]. Data labeled with dissimilar letters differ statistically. Data show significant main ($F_{7,20}=254.9; p<0.0001$), 12 hour food deprivation ($F=254.9, p<0.0001$), Cc ($F=64.34, p<0.0001$), and interaction [suspended feeding and Cc ($F=13.19, p=0.002$); suspended feeding and E ($F=112.30; p = 0.002$)] effects.